Received: 18 September 2017 | Accepted: 18 February 2018

DOI: 10.1111/1365-2435.13087

RESEARCH ARTICLE

Functional Ecology | BRITISH ECOLOGICAL SOCIETY

Structural controls on photosynthetic capacity through juvenile-to-adult transition and needle ageing in Mediterranean pines

Vivian Kuusk[1] | Ülo Niinemets[1,2] | Fernando Valladares[3,4]

[1]Institute of Agricultural and Environmental Sciences, Estonian University of Life Sciences, Tartu, Estonia

[2]Estonian Academy of Sciences, Tallinn, Estonia

[3]LINCGlobal, Departamento de Biogeografía y Cambio Global, Museo Nacional de Ciencias Naturales, MNCN-CSIC, Madrid, Spain

[4]Departamento de Biología y Geología, ESCET, Universidad Rey Juan Carlos, Móstoles, Spain

Correspondence
Ülo Niinemets
Email: ylo.niinemets@emu.ee

Funding information
European Regional Development Fund; Eesti Teadusagentuur, Grant/Award Number: IUT 8-3; Consejo Superior de Investigaciones Cientificas; European Regional Fund, Grant/Award Number: Center of Excellence EcolChange

Handling Editor: Mark Tjoelker

Abstract

1. Needle photosynthetic potentials strongly vary among primary (juvenile) and secondary (adult) needles (heteroblasty) in *Pinus* species, but there is limited understanding of the underlying structural, diffusional and chemical controls.
2. We studied differences in needle photosynthetic characteristics among current-year juvenile and adult needles and among different-aged adult needles in Mediterranean pines *Pinus halepensis* Mill., *P. pinea* L. and *P. nigra* J. F. Arnold subsp. *salzmannii* (Dunal) Franco, hypothesizing that needle anatomical modifications upon juvenile-to-adult transition lead to reduced photosynthetic capacity due to greater limitation of photosynthesis by mesophyll conductance and due to an increase in the share of support tissues at the expense of photosynthetic tissues. We also hypothesized that such alterations occur with needle ageing, but to a lower degree.
3. Photosynthetic capacity per dry mass was 2.4- to 2.7-fold higher in juvenile needles, and this was associated with 3.4- to 3.7-fold greater mesophyll diffusion conductance, 2- to 2.5-fold greater maximum carboxylase activity of Rubisco (V_{cmax}) and 2.2- to 3-fold greater capacity for photosynthetic electron transport (J_{max}). The latter differences were driven by modifications in mesophyll volume fraction and changes in the share of nitrogen between structural and photosynthetic functions. Analogous changes in photosynthetic characteristics occurred with needle ageing, but their extent was less.
4. These results indicate that conifer foliage photosynthetic machinery undergoes a profound change from a fast return strategy in juveniles to slow return stress-resistant strategy in adults and that this strategy shift is driven by modifications in foliage biomass investments in support and photosynthetic functions as well as by varying mesophyll diffusional controls on photosynthesis. Changes in needle morphophysiotype during tree and needle ageing need consideration in predicting changes in tree photosynthetic potentials through tree ontogeny and during and among growing seasons.

KEYWORDS

mesophyll conductance, nitrogen content, photosynthetic capacity, *Pinus halepensis*, *Pinus nigra*, *Pinus pinea*, primary needles, secondary needles

TABLE 1 Influences of tree age and needle age on net assimilation rate (A) and mesophyll diffusion conductance (g_m) expressed per unit dry mass (A_m and $g_{m,m}$) and needle projected area (A_P and $g_{m,P}$), photosynthetic nitrogen use efficiency (E_N, the ratio of A_P and nitrogen content per projected area) and CO_2 drawdown from substomatal cavities to chloroplasts (C_i-C_c) in three Mediterranean *Pinus* species

Species	Tree age class	Needle age	$A_{m,Ci=250}$ ($\mu mol\ g^{-1}\ s^{-1}$)	$A_{P,Ci=250}$ ($\mu mol\ m^{-2}\ s^{-1}$)	E_N ($\mu mol\ g^{-1}\ s^{-1}$)	$g_{m,m}$ ($mmol\ g^{-1}\ s^{-1}$)	$g_{m,P}$ ($mmol\ m^{-2}\ s^{-1}$)	CO_2 drawdown, C_i-C_c ($\mu mol/mol$)
Pinus halepensis	Seedling	(juv)	0.052 ± 0.009^{b}	6.6 ± 0.9^{cd}	4.7 ± 0.6^{cd}	1.19 ± 0.09^{b}	153 ± 11^{c}	44 ± 8^{a}
P. halepensis	Mature	(m0)	0.0222 ± 0.0029^{a}	5.0 ± 0.7^{abcd}	2.51 ± 0.41^{abc}	0.300 ± 0.030^{a}	67 ± 6^{ab}	74 ± 7^{bc}
P. halepensis	Mature	(m1)	0.0126 ± 0.0025^{a}	2.89 ± 0.40^{a}	1.40 ± 0.23^{ab}	0.168 ± 0.025^{a}	38.9 ± 3.7^{a}	73.5 ± 4.5^{bc}
P. nigra	Seedling	(juv)	0.065 ± 0.010^{b}	6.5 ± 0.7^{cd}	7.0 ± 1.2^{d}	1.30 ± 0.11^{b}	133 ± 10^{c}	50 ± 6^{a}
P. nigra	Mature	(m0)	0.0262 ± 0.0009^{a}	6.33 ± 0.28^{cd}	2.51 ± 0.16^{abc}	0.352 ± 0.043^{a}	84 ± 7^{b}	78 ± 9^{bc}
P. nigra	Mature	(m1)	0.0170 ± 0.0014^{a}	4.59 ± 0.37^{abcd}	1.52 ± 0.09^{a}	0.196 ± 0.020^{a}	53 ± 5^{ab}	87.2 ± 2.5^{c}
P. nigra	Mature	(m2)	0.0128 ± 0.0011^{a}	3.60 ± 0.30^{ab}	1.35 ± 0.15^{a}	0.152 ± 0.015^{a}	42.8 ± 4.3^{a}	85 ± 5^{c}
P. pinea	Seedling	(juv)	0.052 ± 0.010^{b}	7.0 ± 0.6^{d}	3.6 ± 0.6^{bc}	1.15 ± 0.24^{b}	155 ± 17^{c}	45.6 ± 2.2^{ab}
P. pinea	Mature	(m0)	0.0195 ± 0.0016^{a}	5.16 ± 0.43^{bcd}	1.62 ± 0.22^{ab}	0.268 ± 0.011^{a}	70.9 ± 3.3^{ab}	72.7 ± 4.8^{bc}
P. pinea	Mature	(m1)	0.0177 ± 0.0030^{a}	4.21 ± 0.36^{abc}	1.33 ± 0.20^{a}	0.185 ± 0.029^{a}	44.3 ± 4.0^{a}	95.7 ± 2.1^{c}
P. pinea	Mature	(m2)	0.0098 ± 0.0012^{a}	3.33 ± 0.37^{ab}	0.95 ± 0.09^{a}	0.120 ± 0.010^{a}	40.5 ± 2.6^{a}	81 ± 6^{c}
F-values for two-way ANOVA (juvenile vs. adult current-year needles)								
Tree age ($F_{1,23}$)			51.4***	5.41*	37.1***	92.2***	88.8***	30.6***
Species ($F_{2,23}$)			0.93ns	0.56ns	5.31*	0.50ns	0.12ns	0.34ns
Tree age × Species ($F_{2,23}$)			0.32ns	0.77ns	2.33ns	0.04ns	2.04ns	0.02ns
F-values for two-way ANOVA (adult needles of different age)								
Needle age ($F_{2,37}$)			19.4***	19.6***	18.7***	33.3***	39.9***	3.33*
Species ($F_{2,37}$)			2.15ns	5.64**	5.79**	2.33ns	4.79*	2.48ns
Needle age × Species ($F_{3,37}$)			1.12ns	0.52ns	1.59ns	0.82ns	0.41ns	2.02ns

The young trees were 2 years old and 0.2–0.3 m tall, and the mature cone-bearing trees were 15–21 m tall at the time of sampling. Needle age codes as: juv—juvenile current year; m0—mature current year; m1—mature 1-year-old; m2—mature 2-year-old. Due to leaf-to-leaf differences in stomatal openness, net assimilation rates were standardized to a common intercellular CO_2 concentration (C_i) of 250 μmol mol^{-1} with the Farquhar et al. (1980) photosynthesis model. n = 4–6 for each average value, except for E_N (n = 3–6 for each average estimate, and n = 19 for the residuals of the F-values for the ANOVA with juvenile vs. adult needles, and n = 26 for the ANOVA with adult needle ages). Different letters show statistical significance among averages for different species and needle age class combinations at $p < .05$ (one-way ANOVA followed by a Tukey post hoc test). For two-way ANOVA, the statistical significance is denoted as: *$p < .05$, **$p < .01$, ***$p < .001$, ns—not significant.

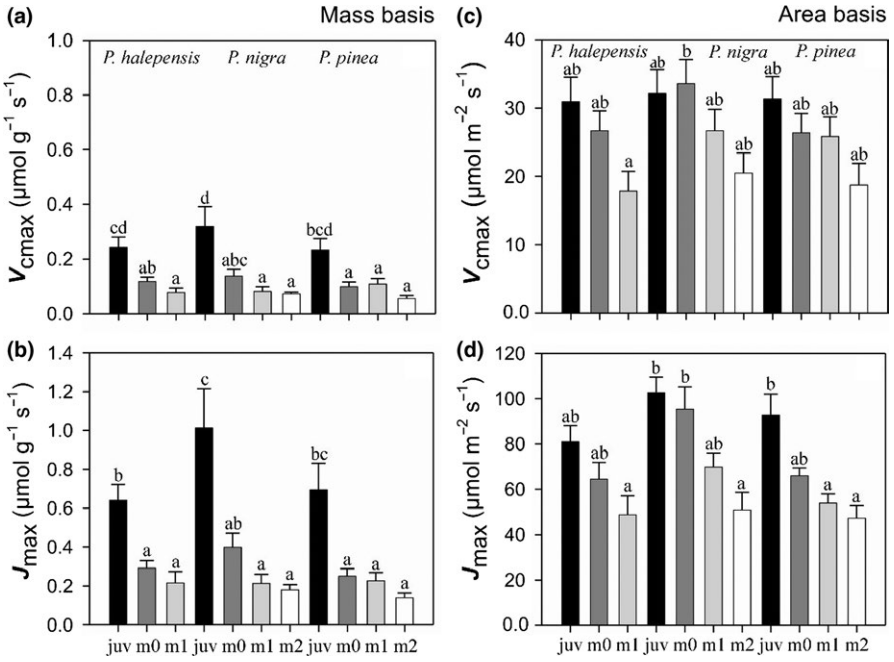

FIGURE 1 Variation in the maximum carboxylase activity of Rubisco (V_{cmax}; a, c) and the capacity for photosynthetic electron transport (J_{max}; b, d) expressed per unit needle dry mass (a, b) and projected needle area (c, d) as driven by needle and tree age in three Mediterranean *Pinus* species. V_{cmax} and J_{max} were derived from net assimilation (A) vs. chloroplastic CO_2 (C_c)–response curves. n = 4–6 for each leaf age × species combination. Table 1 shows corresponding values of net assimilation rate (A) and mesophyll diffusion conductance (g_m). Needle age codes as: juv—juvenile (primary) current year; m0—mature (secondary) current year; m1—mature 1-year-old; m2—mature 2-year-old needles. The juvenile needles were studied in 2-year-old 0.2- to 0.3-m-tall young plants, and the secondary needles in 15- to 21-m-tall cone-bearing mature trees. Different letters denote statistical significance of average values for different species and needle age class combinations at $p < .05$ (one-way ANOVA followed by a Tukey post hoc test). According to two-way ANOVA comparing juvenile and adult current-year needles in different species, tree age effect was significant for a, b and c, species effect for b and d, and tree age × species interaction was not significant in any of the relationships. According to two-way ANOVA comparing adult needle ages in different species, needle age was significant in all cases, species effect for c and d, and needle age × species interaction was not significant in any of the cases (Table 1 for details of the two-way ANOVA models)

1 | INTRODUCTION

Profound modifications in foliage structural and photosynthetic traits occur with increases in tree age and size (Day, Greenwood, & White, 2001; Mediavilla, Herranz, González-Zurdo, & Escudero, 2014; Niinemets, 2002; Niinemets & Kull, 1995; Steppe, Niinemets, & Teskey, 2011; Woodruff, Meinzer, Lachenbruch, & Johnson, 2009). Particularly large trait alterations occur upon juvenile-to-adult transition, a change called heteroblasty (Zotz, Wilhelm, & Becker, 2011). Heteroblastic modifications in foliage morphology are especially large in pine species (Boddi, Bonzi, & Calamassi, 2002; Climent, San-Martín, Chambel, & Mutke, 2011; Kuusk, Niinemets, & Valladares, 2018b; Mediavilla et al., 2014; Pardos, Calama, & Climent, 2009). Juvenile (primary) pine needles are solitary and have different cross-sectional shape, ellipsoidal or rhomboidal, compared to adult (secondary) needles that have semi-elliptical (two-needled species) or sectorial (species with three or more needles in fascicles) shape (Climent, Aranda, Alonso, Pardos, & Gil, 2006; Kuusk et al., 2018b). In addition, needle linear dimensions, thickness and width, and needle dry mass per unit area are typically lower in juvenile needles (Boddi et al., 2002; Kuusk et al., 2018b; Mediavilla et al., 2014; Pardos et al., 2009).

Despite lower needle cross-sectional area, juvenile needles have greater net assimilation rates on both needle area and dry mass basis (Niinemets, 2002), but the mechanisms responsible for greater juvenile needle photosynthesis have not yet been fully resolved. Previous research has indicated that photosynthesis in older and larger conifer trees is more severely limited by stomatal conductance, albeit larger trees also have lower foliage biochemical photosynthesis potentials, maximum carboxylase activity of Rubisco (V_{cmax}) and the capacity for photosynthetic electron transport (J_{max}) (Day et al., 2001; Niinemets, 2002; Räim, Kaurilind, Hallik, & Merilo, 2012; Steppe et al., 2011; Woodruff et al., 2009). It has further been suggested that photosynthesis in structurally more robust needles in older and larger trees is more strongly limited by mesophyll diffusion conductance from substomatal cavities to chloroplasts due to longer effective diffusion path lengths (Niinemets, 2002), but the experimental support to this hypothesis is lacking (Niinemets, Díaz-Espejo, Flexas, Galmés, & Warren, 2009 for a review).

The concept of leaf economics spectrum describes coordinated variations in leaf structure and physiological activity through high return lavish strategy to conservative low return stress-tolerant strategy focusing on three main traits ("core traits"), leaf dry mass per unit area, nitrogen content and photosynthetic capacity (Wright,

TABLE 2 Correlations of needle photosynthetic traits, net assimilation rate (A) and mesophyll diffusion conductance (g_m) expressed per unit needle dry mass (A_m and $g_{m,m}$) and needle projected area (A_P and $g_{m,P}$), and photosynthetic nitrogen use efficiency (E_N, the ratio of A_P and nitrogen content per projected area) with needle structural and chemical traits across all needle and tree ages in three Mediterranean species (Pearson correlation coefficients)

Structural/chemical traits	Physiological traits				
	$A_{m,Ci=250}$	$A_{P,Ci=250}$	E_N	$g_{m,m}$	$g_{m,P}$
Fraction in epidermal tissues	−0.367*	−0.378**	−0.313*	−0.367**	−0.365*
Fraction in central cylinder	−0.783***	−0.541***	−0.770***	−0.796***	−0.650***
Total mechanical fraction	−0.786***	−0.605***	−0.754***	−0.780***	−0.683***
Total mesophyll faction	0.774***	0.639***	0.738***	0.789***	0.713***
Mesophyll fraction without air space	0.646***	0.544***	0.605***	0.660***	0.587***
Dry mass per unit projected area ($M_{A,P}$)	−0.743***	−0.523***	−0.762***	−0.743***	−0.650***
Volume to projected area ratio (V/S_P)	−0.639***	−0.397**	−0.717***	−0.659***	−0.567***
Density (D)	−0.422***	−0.316*	−0.762***	−0.401**	−0.335**
Dry to fresh mass ratio ($R_{D/F}$)	−0.591***	−0.648***	−0.561***	−0.581***	−0.655***
Nitrogen content per dry mass (N_m)	0.330*	0.493***	0.061^{ns}	0.337*	0.437**
Nitrogen content per projected area ($N_{A,P}$)	−0.558***	-0.213^{ns}	−0.663***	−0.569***	−0.397**

n = 46 for the combinations of photosynthesis vs. tissue volume fractions and chemical traits and for all correlations with E_N, and n = 57 for the other traits. Statistical significance as in Table 1.
Tissue mechanical fraction is the sum of the needle volume fractions in epidermal tissues (epidermis and hypodermis) and central cylinder. Net assimilation rates were standardized for all leaves to a common intercellular CO_2 concentration (C_i) of 250 μmol/mol as in Table 1. Additional methods for structural trait estimation are provided in Kuusk et al. (2018b), and all data accompanying this article are available from the Dryad Digital Repository (Kuusk et al., 2018a). Statistical significance as in Table 1.

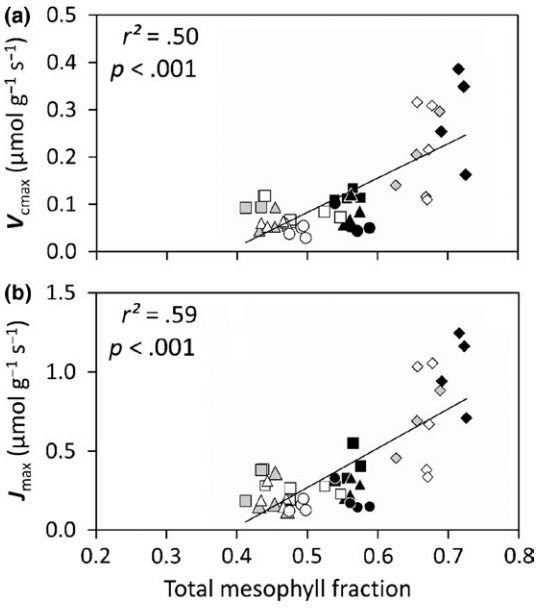

FIGURE 2 Relationships of maximum carboxylase activity of Rubisco (V_{cmax}; a) and capacity for photosynthetic electron transport (J_{max}; b) per unit dry mass with mesophyll volume fraction in three Mediterranean *Pinus* species. Data for all species and needle and plant ages pooled were fitted by linear regressions. Mesophyll volume fraction is given without intercellular air space (Kuusk et al., 2018b for details about its estimation). Different symbols as: grey = *Pinus halepensis*, black = *Pinus nigra*, white = *Pinus pinea*; diamonds = juv, squares = m0, triangles = m1, circles = m2. Figure 1 for the definition of age codes

Reich, et al., 2004). The economics spectrum relationships have been developed by pooling plants with varying age (Kattge et al., 2011;). So far, possible implications of juvenile-to-adult transition on leaf trait relationships have not been explored and the traits in seedlings and adult plants are considered as parts of the same general economics spectrum. However, there is a strategy shift from juvenile physiologically active and less stress-tolerant strategy to adult more sclerophyllous higher stress tolerance strategy (Climent, San-Martín, et al., 2011; Harper, 1989; Karban & Thaler, 1999; Kuusk et al., 2018b; Mediavilla et al., 2014; Pardos et al., 2009), suggesting that heteroblastic changes could alter the trait relationships. Mesophyll diffusion conductance and fractional tissue distribution do not belong to the "core" traits of the leaf economics spectrum as initially defined (Wright, Reich, et al., 2004), but they both can alter foliage photosynthetic capacity at given leaf dry mass per unit area and nitrogen content. Existence of a trade-off between structural and photosynthetic functions could mean that leaf photosynthetic capacity changes more at a given dry mass per unit area and nitrogen content than predicted by the broadleaf economics spectrum relationships.

We studied modifications in foliage photosynthetic characteristics upon juvenile-to-adult transition in three Mediterranean pine species—*Pinus halepensis* Mill., *P. pinea* L. and *P. nigra* J. F. Arnold subsp. *salzmannii* (Dunal) Franco. Differently from European pines in wetter climates where juvenile needles are present in up to 1-year-old seedlings, young Mediterranean pines typically carry juvenile needles longer, for 2–3 years (Climent, San-Martín, et al.,

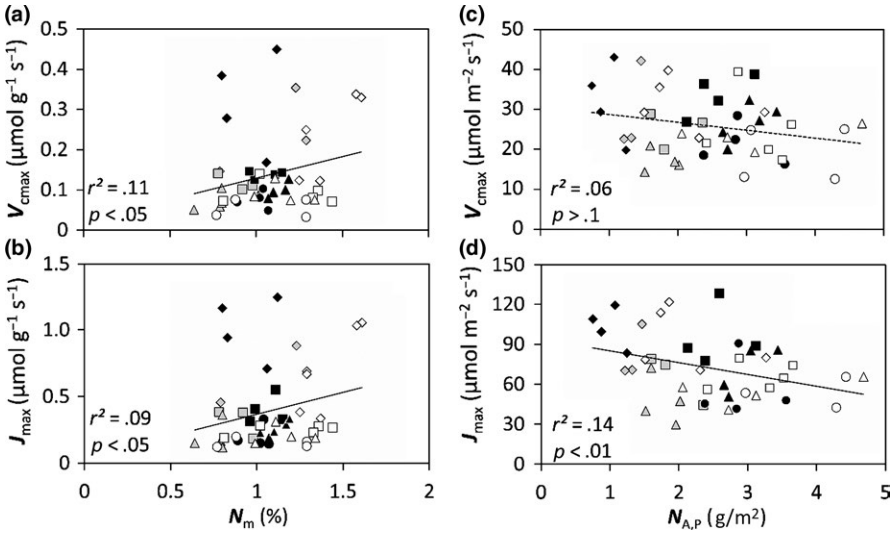

FIGURE 3 Correlations of maximum carboxylase activity of Rubisco (V_{cmax}; a, c) and capacity for photosynthetic electron transport (J_{max}; b, d) per unit dry mass (a, b) and projected area (c, d) with nitrogen content per unit dry mass (a, b) and per unit projected area (c, d) in three Mediterranean *Pinus* species. Linear regressions were used to fit data (all species and needle and plant ages pooled). Symbols as in Figure 2

2011), suggesting that heteroblastic differences constitute an important seedling adaptation in Mediterranean highly stressful environments. We have previously reported that juvenile needles have lower needle density, greater fraction of mesophyll tissue in needles, thinner mesophyll cell walls and greater chloroplast to exposed mesophyll cell wall surface area, while secondary needles in adult trees are characterized by the opposite suite of these traits (Kuusk et al., 2018b). Here, we hypothesized that these trait differences result in concomitant variations in needle photosynthetic capacity and that the alteration in needle photosynthetic potentials is driven by the trade-off between support and photosynthetic investments demonstrated in Kuusk et al. (2018b), and furthermore, that the greater structural robustness in adult needles is associated with a stronger limitation of photosynthesis by mesophyll diffusion conductance.

Needle age also influences foliage structural traits and nutrient content (Mediavilla et al., 2014; Niinemets, 2002; Niinemets, García-Plazaola, & Tosens, 2012; Teskey, Grier, & Hinckley, 1984; Weiskittel, Temesgen, Wilson, & Maguire, 2008), but the effects of these modifications on age-dependent changes in needle photosynthetic potentials are still not fully resolved. Thus, in mature trees we studied variation in foliage photosynthetic potentials in non-senescent adult current-year, 1-year-old and 2-year-old needles. We hypothesized that the age-dependent changes in photosynthetic activity with needle age are also driven by changes in mesophyll conductance and accumulation of support tissues, but that trait changes with needle age are comparatively less extensive than modifications upon juvenile-to-adult transition.

2 | MATERIAL AND METHODS

2.1 | Measurement sites and plant sampling

Full details of study sites, plants and plant sampling are provided in Kuusk et al. (2018b). In short, the study was conducted in sites with continental Mediterranean climate characterized by hot dry summers and relatively cold dry winters. Adult cone-bearing trees were investigated at Alto Tajo Natural Park, Central Spain (Guadalajara, Castilla-La Mancha, 40.8480°N, 2.1812°W, mean elevation 950 m). The mean annual rainfall at the site is 490 mm and mean annual temperature 10.2°C (Molina de Aragón whether station, 40.8444°N, 1.8853°W, elevation 1,063 m). In each species, five mature plants at full sunlight were randomly selected for sampling. The trees were 90–100 years old and 15–21 m tall (Kuusk et al., 2018b for species averages). Terminal branchlets without cones (one branch from each individual tree) were taken from the southern part of the upper canopy (average seasonal integrated quantum flux density of ca. 40 mol m^{-2} day^{-1}) to minimize shading effects on foliage characteristics (Gebauer et al., 2011; Niinemets, Keenan, & Hallik, 2015) in October 2005 and in August 2006. The branches were cut under water, and the cut ends were kept in water and transported to the laboratory for gas-exchange and anatomical measurements. Previous studies have indicated that use of cut branches allows for obtaining representative estimates of foliage gas-exchange characteristics, except stomatal conductance that can differ from the values in the field (e.g., Niinemets, Cescatti, Rodeghiero, & Tosens, 2005; Peñuelas et al., 2010).

There were very few seedlings at the field site, as is common in Mediterranean forests, and the seedlings in the understorey of mature trees were shaded and no recent clear-cut or disturbed areas were available. Therefore, to study juvenile foliage, 2-year-old juvenile trees were obtained from a local nursery at El Seranillo Forestry Center, Guadalajara. They were grown in 5-L pots filled with a mixture (4:4:1:1, v/v) of compost, vermiculite, perlite and sand at the Museo Nacional de Ciencias Naturales (CSIC) in Madrid, Spain (40.440°N, 3.690°W, elevation 682 m). The pots were buried in the soil such that pot soil temperature was ambient, and were exposed to full sunlight (average daily integrated photosynthetic quantum flux density of 41 mol m^{-2} day^{-1}). For the measurements, current-year juvenile foliage formed in the new growth conditions was used. Obviously, the current experimental design introduces unknown sources of variation due to somewhat different growth

environments for mature and juvenile trees, but such problems are inherent to comparisons of different sized and aged plants. Kuusk et al. (2018b) provide a thorough discussion of potential disadvantages and advantages of our design. Because foliage shading is quantitatively the most important environmental factor affecting leaf structure and function (Niinemets et al., 2015; Keenan & Niinemets, 2016; Poorter, Niinemets, Poorter, Niinemets, Poorter, Wright, & Villar, 2009), we considered our design more appropriate than the alternative of comparing high light exposed adult and shaded understorey juvenile plants. We note that the experimental design used here is analogous to studies carried out along the chronosequence of different stands and is also appropriate from an ecological perspective as shade-intolerant Mediterranean pine seedlings cannot persist in the understorey, and can reach the canopy only once a major gap forms in the canopy (Climent, San-Martín, et al., 2011; Kuusk et al., 2018b).

In adult trees carrying secondary needles, current-year, 1-year-old and 2-year-old needles were measured, except for *P. halepensis* that supported only two needle age classes due to shorter needle life span. In the juveniles, where the canopy was chiefly made up of primary current-year needles, only primary needles formed at the growth conditions were studied. In 2005, five juvenile plants, and four to five branches from adult trees from each studied species were measured for foliage photosynthesis characteristics. In 2006, additional branches from adult trees were measured: two branches from *P. halepensis*, three branches from *P. pinea* and three branches from *P. nigra*. In total, 24 branches from adult trees (from eight trees of each species) and 15 juvenile plants (five of each species) were used. Thus, for each tree age × leaf age × species combination, altogether four to six samples (on average 5.2) were measured.

2.2 | Needle gas-exchange measurements

Gas-exchange measurements were carried out with a Li-Cor 6400 portable gas-exchange system (Version 5; Li-Cor, Inc., Lincoln, NE, USA) using the 2-cm^2 leaf chamber fluorimeter measurement head. Needles were enclosed side by side to avoid overlap between the needles and standard environmental conditions of chamber block temperature of 25°C, ambient CO_2 concentration of 400 μmol/mol, quantum flux density of 2,200 μmol m^{-2} s^{-1} (10% blue light) were established, and the leaves were conditioned in the chamber until stomata opened and steady-state gas-exchange rates were established, typically in 30 min after needle enclosure. After reaching the steady state, the CO_2–response curve was measured first, followed by the light–response curve. In the case of the CO_2–response curve, ambient CO_2 concentrations were prepared in sequence of 400, 600, 900, 1,200, 1,600, 200, 300, 200 and 50 μmol/mol and steady-state rates of net assimilation were recorded at each CO_2 concentration. In the case of the light–response curve, light intensity was changed in the sequence of 1,200, 1,800, 800, 500, 250, 125, 80, 30 and 0 μmol m^{-2} s^{-1} and again steady-state rates at each light level were recorded. At the end of the measurements, light was switched off and the rate of dark respiration was measured when the cuvette temperature stabilized and leaf gas-exchange reached a steady state, typically in 4–5 min after switching off the light. At each CO_2 and light level, a saturating light flash of 6,800 μmol m^{-2} s^{-1} was given to estimate the effective quantum yield of photosystem II:

$$\Phi_{PSII} = (F'_m - F_s)/F'_m, \quad (1)$$

where F'_m is the maximum and F_s the steady-state fluorescence yield of light-adapted leaves (Genty, Briantais, & Baker, 1989). From these measurements, the rate of photosynthetic electron transport from chlorophyll fluorescence, J_{ETR}, was calculated as:

$$J_{ETR} = 0.5\zeta\Phi_{PSII}Q, \quad (2)$$

where Q is the quantum flux density and ζ is the leaf absorptance (an average value of 0.9 was used in this study in accordance with estimates of quantum yields obtained from light–response curves).

2.3 | Estimations of Farquhar, von Caemmerer, and Berry (1980) photosynthesis model characteristics and mesophyll conductance

Before calculation of foliage gas-exchange rates, the data were corrected for CO_2 and water vapour diffusion leaks according to Rodeghiero, Niinemets, and Cescatti (2007) using diffusion leak coefficients of 0.445 μmol/s for CO_2 and 5.11 μmol/s for water vapour. After diffusion corrections, all gas-exchange rates were calculated according to von Caemmerer and Farquhar (1981) using the leaf areas estimated from leaf anatomical measurements as detailed in the next section (between 1.5 and 2 cm^2 projected leaf area was included in the leaf chamber). Farquhar et al. (1980) model of photosynthesis was first fitted to net assimilation (A) vs. intercellular CO_2 (C_i)–response curves and the apparent values of the maximum carboxylase activity of ribulose-1,5-bisophosphate carboxylase/oxygenase (Rubisco, $V_{cmax,Ci}$) and the capacity for photosynthetic electron transport ($J_{max,Ci}$) were estimated as in Niinemets et al. (2005) using the Rubisco kinetic characteristics from Bernacchi, Singsaas, Pimentel, Portis, and Long (2001).

Based on gas-exchange and chlorophyll fluorescence measurements (Harley, Loreto, di Marco, & Sharkey, 1992), mesophyll diffusion conductance to CO_2 was estimated as:

$$g_m = \frac{A}{C_i - \frac{\Gamma^*[J_{ETR}+8(A+R_d)]}{J_{ETR}-4(A+R_{d)}}}, \quad (3)$$

where Γ^* is the hypothetical CO_2 compensation point in the absence of dark respiration and R_d is the non-mitochondrial respiration rate in light (taken as half of the dark respiration rate, e.g., Way & Yamori, 2014; Niinemets, 2014). Using the values of g_m, chloroplastic CO_2 concentrations corresponding to each C_i value were calculated as $C_c = C_i - A/g_m$ and A vs. C_c–response curves were obtained. Farquhar et al. (1980) photosynthesis model was re-fitted to these data, and C_c-based estimates of foliage photosynthetic potentials ($V_{cmax,Cc}$) and $J_{max,Cc}$) were determined.

As at the given chamber block temperature, leaf temperatures varied somewhat (between 24 and 30°C), both C_i- and C_c-based

estimates of foliage biochemical potentials were standardized to a common temperature of 25°C using the shape of the specific activity of Rubisco of Niinemets and Tenhunen (1997) for V_{cmax}, and the shape of J_{max} temperature–response curve characteristic to Mediterranean species (temperature optimum of 39.7°C, Niinemets et al., 2002). As V_{cmax} and J_{max} calculated from C_i and C_c curves were strongly correlated (r^2 = .82 for V_{cmax} and r^2 = .92 for J_{max}, p < .001 for both), we only demonstrate data for C_c-based estimates.

Branch-to-branch differences in leaf temperature were also associated with a certain variation in vapour pressure deficit (1.41–2.82 kPa, average ± SE = 2.050 ± 0.013 kPa) and degree of stomatal limitation of photosynthesis (as evident in a certain variation in C_i values at the reference ambient CO_2 concentrations common in experiments using cut twigs). Thus, the parameterized Farquhar et al. (1980) photosynthesis model was used to obtain standardized estimates of leaf net assimilation rates independent of stomatal conductance at a C_i value of 250 μmol/mol as in Niinemets, Wright, and Evans (2009).

2.4 | Calculation of leaf area enclosed in the gas-exchange cuvette and foliage chemical and structural data

After photosynthesis measurements, needles enclosed in the gas-exchange cuvette were harvested and total needle length (L), the length of enclosed needle section (L_E), width (W) and thickness (T) were measured with Starrett Digital callipers (model 727, L. S. Starrett Company, Athol, MA, USA). From these measurements, average needle projected area, S_P, was calculated as WL, and needle projected area enclosed in the chamber as the sum of the products L_EW of individual needles enclosed in the chamber ($\sum_{i=1}^{i=n} L_{E,i}W_i$, where n is the number of needles enclosed in the chamber).

Measurements of needle volume (V), total to projected area ratio (S_T/S_P), dry mass per unit projected ($M_{A,P}$) and total ($M_{A,T}$) needle area, density (D, needle volume per dry mass), volume to projected area ratio, V/S_P, dry to fresh mass ratio, $R_{D/F}$, nitrogen content per unit projected ($N_{A,P}$) and total ($N_{A,T}$) needle area, tissue volume fractions in support (volume fractions in epidermis, hypodermis and central cylinder) and photosynthetic mesophyll, and needle ultrastructural characteristics are described in Kuusk et al. (2018b). Foliage photosynthetic characteristics per total area were calculated as the values per projected area divided by S_T/S_P. Needle photosynthetic characteristics per dry mass were calculated as the values expressed per projected area divided by $M_{A,P}$. Area- and mass-based physiological traits characterize different facets of leaf functioning. Dry mass-based foliage photosynthetic potentials characterize the photosynthetic return on biomass investment in leaves, and area-based capacities indicate the integrated outcome of differences in leaf structure and photosynthetic capacity of single mesophyll cells (Niinemets & Sack, 2006; Onoda et al., 2017; Wright, Reich, et al., 2004). Expressions of g_m per area and dry mass both characterize the extent to which CO_2 diffusion from intercellular air space to chloroplasts limits photosynthesis, but given that both intercellular and chloroplastic CO_2 concentrations are leaf volume-weighted estimates, diffusion limitations generally scale more strongly with g_m per dry mass (Niinemets, Díaz-Espejo, et al., 2009).

2.5 | Statistical analyses

Differences in average trait values among study years, needle ages and among adult and juvenile trees were tested by ANOVA followed by Tukey's post hoc tests with STATISTICA 6 (StatSoft, Inc., Tulsa, USA) and R 3.1.1 with default packages (R Development Core Team, 2012) as in Kuusk et al. (2018b). As the year of study was not significant in any of the analyses, it was removed from the final analyses. Two-way ANOVAs were used to test for effects of species and heteroblasty among current-year needles, and effects of species and needle age among adult needles. Relationships among leaf traits were explored by linear (Pearson) correlation and nonlinear regression analyses. All statistical effects were considered significant at p < .05. The data accompanying this article are available from the Dryad Digital Repository (Kuusk, Niinemets, & Valladares, 2018a).

3 | RESULTS

3.1 | Tree and needle age, and species-dependent changes in needle photosynthetic characteristics

Foliage net assimilation rate per unit dry mass (A_m) was greater for juvenile than for adult current-year needles (Table 1). Net assimilation rate per unit projected area (A_P), the product of needle dry mass per projected area ($M_{A,P}$) and A_m was less variable, but juvenile needles nevertheless had a greater A_P when all species were analysed together (Table 1). Analogously to A_m, nitrogen use efficiency (the ratio of A_m to N_m, E_N) was significantly greater in juvenile than in adult current-year needles (Table 1).

Analysis of needle biochemical potentials, maximum carboxylase activity of Rubisco (V_{cmax}) and photosynthetic electron transport (J_{max}) derived from the net assimilation vs. chloroplastic CO_2 (C_c)–response curves indicated that juvenile needles had greater V_{cmax} and J_{max} per unit dry mass than adult current-year needles (Figure 1a,b for species-specific differences and Figure S1A,B in Supporting Information for all species pooled). The estimate of photosynthetic electron transport rate from chlorophyll fluorescence (J_{ETR}, Equation 2) per dry mass was also greater for juvenile that for adult current-year needles (p < .001). Again, V_{cmax} and J_{max} per unit projected area varied less (Figures 1c,d, and S1D,E), but J_{max} per unit projected area was greater in juvenile than in adult current-year needles (Figures 1d and S1E).

Mesophyll diffusion conductance (g_m) was greater in juvenile than in adult current-year needles when expressed both per unit dry mass and projected area (Table 1, Figure S1C,F). The CO_2 drawdown from substomatal cavities to chloroplasts, C_i-C_c, was lower for juvenile than for adult current-year needles (Table 1, Figure S1C).

Analysis of the needle age effects on adult needles across all species indicated that foliage net assimilation rates, foliage biochemical potentials, V_{cmax} and J_{max}, and g_m both per unit dry mass and area, and nitrogen use efficiency generally decreased with increasing

needle age (Figures 1 and S1, Table 1). Needle age effects on CO_2 drawdown were less, but still significant (Table 1, Figure S1C).

Both tree age and needle age-dependent modifications occurred similarly in all species (no significant species × tree age and species × needle age interactions, Figure 1 and Table 1), but species differed in average values of some photosynthetic traits (E_N, J_{max} per unit area and dry mass for current-year juvenile and adult needles, and A_m, A_P, and area-based g_m, V_{cmax} and J_{max} for different-aged adult needles; Figure 1 and Table 1). This mainly reflected superior photosynthetic characteristics in *P. nigra* (Figure 1 and Table 1).

3.2 | Correlations of leaf photosynthetic characteristics with leaf structural and chemical traits

Foliage net assimilation rate and underlying partial determinants, E_N, V_{cmax}, J_{max} and g_m, scaled positively with needle mesophyll volume fraction (measured as the fraction of needle mesophyll in needle cross-section) and negatively with volume fractions of mechanical tissues (Figure 2a,b; Table 2), whereas the correlations were stronger for mass-based photosynthetic characteristics (Table 2; r^2 = .26 for V_{cmax} and r^2 = .36 for J_{max} expressed per unit area vs. total mesophyll fraction, p < .001 for both). Needle traits characterizing leaf structural robustness, $M_{A,P}$, density (D) and volume to projected surface area ratio (V/S_P; $M_{A,P} = DV/S_P$, and needle dry to fresh mass ratio ($R_{D/F}$) were generally also negatively associated with both area- and mass-based V_{cmax} and J_{max} (p < .01 for all, except for V_{cmax} per area vs. D, p > .07). Again, these negative relationships were stronger for mass-based (Table 2; for the four structural traits, average r^2 = .35 for relationships with V_{cmax} and r^2 = .40 for relationships with J_{max}) than for area-based (Table 2; average r^2 = .15 for relationships with V_{cmax} and r^2 = .25 for relationships with J_{max}) V_{cmax} and J_{max}.

There were weak positive correlations of mass-based foliage photosynthetic characteristics, A, g_m (Table 2) and V_{cmax} (Figure 3a) and J_{max} (Figure 3b), with foliage nitrogen content per dry mass. However, the correlations of area-based characteristics with nitrogen content per area were even non-significant or negative (Table 2; Figure 3c,d). In fact, photosynthetic nitrogen use efficiency was a stronger determinant of net assimilation rate than nitrogen content ($A_m = E_N N_m$ and $A_P = E_N N_{A,P}$; r = .92 for A_m vs. E_N and r = .71 for A_P vs. E_N, p < .001 for both). Higher nitrogen use efficiency was associated with enhanced mesophyll diffusion conductance (r = .83 for mass-based g_m vs. E_N and r = .68, for area-based g_m vs. E_N, p < .001 for both).

4 | DISCUSSION

4.1 | Heteroblastic changes in needle photosynthesis

The results of this study collectively demonstrate important differences in foliage photosynthetic potentials and mesophyll conductance among juvenile and different-aged adult needles and that these differences primarily result from modifications in needle structure and the share of support and assimilative tissues. Although for the current dataset, heteroblasty only weakly affected needle nitrogen content per dry mass (Kuusk et al., 2018b), foliage net assimilation rate per dry mass standardized to a common intercellular CO_2 concentration (A_m) was strongly enhanced, 2.4- to 2.7-fold in the juvenile needles of the three pine species studied (Table 1). Net assimilation rate per projected area (A_P), the product of A_m and needle dry mass per unit projected area ($M_{A,P}$), was also moderately greater in juvenile needles (Table 1), indicating that the heteroblastic changes in mass-based photosynthetic capacity, both due to changes in tissue distribution between assimilative and structural tissues and in photosynthetic capacity of individual mesophyll cells, were quantitatively greater than needle biomass accumulation per area. An enhanced assimilation rate per unit foliage biomass implies that the juvenile foliage has a shorter time to pay back the carbon cost used for foliage construction. Thus, juveniles have a greater carbon availability for growth of new biomass, thereby importantly contributing to their early growth and recruitment (Climent, Chambel, Pardos, Lario, & Villar-Salvador, 2011; Climent, San-Martín, et al., 2011; Mediavilla et al., 2014).

Similarly to the current study, a decrease of A_m with increasing tree age and size has been consistently observed in conifers (Day et al., 2001; Mediavilla et al., 2014; Miller, Eddleman, & Miller, 1995; Niinemets, 2002; Räim et al., 2012; Steppe et al., 2011; Woodruff et al., 2009). As observed in our study (Figure 3), this decrease is often associated with much lower variation in foliage nitrogen content per dry mass among different-aged and sized trees (Day et al., 2001; Juárez-López, Escudero, & Mediavilla, 2008; Mediavilla et al., 2014; Niinemets, 2002). Area-based net assimilation rate also typically decreases with increasing tree age and size in conifers (Day et al., 2001; Greenwood, Ward, Day, Adams, & Bond, 2008; Niinemets, 2002; Räim et al., 2012; Steppe et al., 2011), but as also observed in our study (Table 1), the decrease is typically less than in the mass-based rate. Furthermore, quantitatively, heteroblastic modifications in foliage photosynthesis rate are much greater than changes in mass- and area-based photosynthesis rates due to the gradual ontogenetic drift in mature plants (our study vs., e.g., Niinemets, 2002; Räim et al., 2012; Steppe et al., 2011; Woodruff et al., 2009).

It has been suggested that the reduction in the assimilation rate in older trees reflects mainly changes in stomatal conductance (Greenwood et al., 2008; Yoder, Ryan, Waring, Schoettle, & Kaufmann, 1994), but there is evidence that the reduction in stomatal conductance is not the only factor responsible for the decline in photosynthesis rate with tree age (Niinemets, 2002; Räim et al., 2012). In fact, older plants might have an even greater stomatal conductance, but still reduced photosynthesis rate (Day et al., 2001). As our study demonstrated, higher net assimilation rate at a given intercellular CO_2 concentration in juvenile needles was associated both with enhanced biochemical photosynthesis capacities, V_{cmax} and J_{max} (Figures 1 and S1), and enhanced mesophyll diffusion conductance (g_m, Table 1, Figure S1) that affects net assimilation rate by altering the chloroplastic CO_2 concentration (C_c). Mesophyll conductance and foliage photosynthetic capacity can vary in a

coordinated manner such that the CO_2 drawdown from substomatal cavities to chloroplasts, C_i–C_c = A/g_m, is invariable (Evans & Loreto, 2000). However, this is typically not the case across species with varying structure, and C_i–C_c is often greater, and accordingly, g_m-limitation of photosynthesis is more severe in species with more robust foliage structure (Onoda et al., 2017; Tomás et al., 2013; Tosens, Niinemets, Westoby, & Wright, 2012; Veromann, Tosens, Laanisto, & Niinemets, 2017). Our study demonstrated that C_i–C_c was lower in juvenile needles (Table 1, Figure S1), indicating that the mesophyll diffusion limited the rate of photosynthesis to a lower extent in juvenile needles. Such a lower control of photosynthesis by g_m and accordingly, a greater efficiency of use of resources invested in photosynthetic machinery in younger plants has been hypothesized (Niinemets, 2002), but to our knowledge, this had not yet been experimentally confirmed. At the ultrastructural level, greater g_m-limitation of photosynthesis in adult trees was associated with thicker cell walls in *P. nigra* and *P. pinea* and with lower chloroplast to exposed mesophyll surface area ratio in *P. halepensis* (Kuusk et al., 2018b), indicating that the effective diffusion pathway lengths were indeed greater in secondary needles in adult trees than in primary needles in young trees.

Given the frequent and severe drought and temperature stress conditions in Mediterranean environments and sustained biotic stress pressure, the lack of foliage robustness can be a significant limitation to survival of juvenile plants and can explain why successful seedling establishment in Mediterranean conditions can occur only in favourable years with moderate stress conditions (Braza & García, 2011; Prévosto, Gavinet, Ripert, & Fernandez, 2015). Therefore, we suggest that the main advantage of juvenile needles is more effective photosynthesis, which provides the young seedling with necessary carbon building blocks for establishing extensive root systems and later on for development of more durable adult needles which are more resistant to mechanical stress and more tolerant to drought.

4.2 | Modifications in foliage photosynthetic characteristics with needle age

Older needles of the three studied pine species had significantly lower photosynthesis rate per unit needle dry mass and area (Table 1). The reduction in mass-based photosynthesis rate is a characteristic age-dependent change (Oleksyn et al., 1997; Teskey et al., 1984), but there is a variability in the age-dependent changes in area-based photosynthesis (Jensen, Warren, Hanson, Childs, & Wullschleger, 2015; Niinemets, 2002; Tissue, Griffin, Turnbull, & Whitehead, 2001). This variability is driven by differences in how the components of A_P vary with leaf age. For the current dataset, the relative magnitude of the age effects on A_m (1.7-2-fold reduction in our study, Table 1) was greater than on dry mass per unit area (1.1- to 1.3-fold increase for $M_{A,P}$) (Kuusk et al., 2018b), resulting in a significant reduction in A_P with leaf age (Table 1).

The age-dependent reduction in A_m has been associated with a decrease in foliage nitrogen content per dry mass (Oleksyn et al., 1997) that is expected to lead to concomitant reductions in the foliage photosynthetic potentials V_{cmax} and J_{max} (Ethier, Livingston, Harrison, Black, & Moran, 2006; Warren, 2006). Although changes in needle age were primarily associated with reductions in foliage biochemical potentials in our study (Figures 1 and S1A–D), the age effects on foliage nitrogen content were not significant (Kuusk et al., 2018b) in agreement with several other studies demonstrating moderate or minor differences in N_m in needles of different age (Ethier et al., 2006; Warren, 2006). A reduction in V_{cmax} and J_{max} at given N_m might reflect a change in the share of foliage nitrogen distribution between photosynthetic and structural functions (e.g., Warren & Adams, 2000). Especially in sclerophyllous species, a large fraction of foliage nitrogen is associated with cell walls (Dong et al., 2015; Hikosaka & Shigeno, 2009; Onoda et al., 2017; Takashima, Hikosaka, & Hirose, 2004), and given the age-dependent reduction in V_{cmax} and J_{max} observed in our study, it is likely that this fraction increased with increasing leaf structural robustness in ageing needles. It has also been suggested that Rubisco becomes progressively inactivated with increasing needle age, explaining partly the age-dependent reduction in V_{cmax} (Ethier et al., 2006; Warren, 2006).

Increases in leaf age also resulted in a reduction in mesophyll diffusion conductance (Table 1, Figure S1C,F) as observed in several evergreen species (Ethier et al., 2006; Niinemets et al., 2005; Warren, 2006). Given that the decrease in g_m was associated with concomitant increases in the CO_2 drawdown C_i-C_c (Table 1, Figure S1C), reduced g_m indeed limited photosynthesis more in older leaves. Such a greater limitation of photosynthesis by within-leaf diffusion in older leaves has been observed previously in several Mediterranean broadleaved evergreen species (Niinemets et al., 2005). Lower g_m in older needles in our study was associated with longer diffusion pathways due to increases in needle cross-sectional dimensions and lower chloroplast to exposed mesophyll surface area (Kuusk et al., 2018b), and possibly also with lower cell wall porosity of more strongly lignified cell walls in older needles.

4.3 | The implications of the trade-offs between structural and functional investments for foliage photosynthesis

In addition to greater g_m-limitation, more robust secondary needles in mature trees had a lower needle volume fraction in photosynthetic mesophyll (Kuusk et al., 2018b). Such a difference was directly associated with foliage photosynthetic capacity across all data, as the fractional investment in mesophyll was strongly correlated with foliage net assimilation rate (Table 2). Furthermore, the positive correlations with mesophyll volume fraction and foliage photosynthetic potentials (Figure 2) suggest that needles with greater mesophyll volume fraction indeed had greater concentrations of photosynthesizing enzymes.

The mass-based photosynthesis rate varied more among juvenile and adult needles (2.3–2.7-fold, Table 1) than the mesophyll volume fraction (1.3–1.5-fold, Kuusk et al., 2018b), partly reflecting concomitant changes in mesophyll diffusion conductance with tree

age (Table 1). Nevertheless, the photosynthetic potentials (V_{cmax} and J_{max}; Figures 1a,b and S1A,B) that are not directly affected by g_m also varied somewhat more than mesophyll volume fraction. Given the moderate increase of N_m with increasing mesophyll volume faction (Kuusk et al., 2018b), a greater variation in V_{cmax} and J_{max} suggests a positive scaling of nitrogen investments in photosynthetic machinery with mesophyll volume fraction. Indeed, a strong positive correlation was observed between mesophyll volume fraction and nitrogen use efficiency (Table 2).

Species differences in adult needle photosynthesis were small in our study (Table 1), indicating that the moderate species variation in mesophyll volume fraction did not affect needle photosynthetic activity to a large extent. This suggests a certain compensation resulting from species differences in nitrogen content, *P. halepensis* < *P. nigra* ≤ *P. halepensis* (Kuusk et al., 2018b) and in nitrogen use efficiency (Table 1).

4.4 | Weak relationships of foliage photosynthetic characteristics with nitrogen content

Leaf economics spectrum (Wright, Reich, et al., 2004) is a concept describing the covariation of suites of leaf traits across the whole range of strategies from a low return stress-tolerant (low A_m and N_m, high M_A) to a high return, luxurious (high A_m and N_m, low M_A) strategy. The three most prominent relationships in the leaf economics spectrum are the positive correlation between A_m and N_m and negative correlations between A_m and M_A, and N_m and M_A (Wright, Reich, et al., 2004). Across all the data in our study, the negative correlation between A_m and $M_{A,P}$ was highly significant (Table 2), but A_m and N_m were weakly correlated and the correlations of N_m vs. $M_{A,P}$ and $M_{A,T}$ were not significant. It has been suggested that due to inherent inter- and intraspecific variability, broad relationships might not simply be evident within datasets covering only part of the economics spectrum, for example, within the data coming from the low or fast return ends of the economics spectrum (Reich, 1993; Wright, Groom, et al., 2004). On the other hand, it has been argued that different combinations of traits can drive vegetation performance in different parts of the economics spectrum, and thus, although contrasting, "local" relationships can have important functional implications (Diemer, Körner, & Prock, 1992; Niinemets, 2015).

The Mediterranean pines studied here are located at the low return end of the economics spectrum, but nevertheless, variation in foliage photosynthetic capacity, leaf structure and nitrogen content was extensive (Kuusk et al., 2018b; Table 1). However, needle age- and plant age-dependent variations within this dataset primarily affected A_m and $M_{A,P}$ and $M_{A,T}$ and much less N_m, and the key trait explaining the variation of A_m at given N_m was the nitrogen use efficiency which reflects nitrogen distribution among photosynthetically active and non-active leaf functions and the efficiency with which photosynthetic proteins are engaged, that is, mesophyll conductance and the degree of activation of rate-limiting proteins (Onoda et al., 2017). Both the heteroblastic change and needle ageing were associated with lower fractions of nitrogen invested in photosynthetic functions and reduced mesophyll conductance in structurally more robust needles (Table 1). In fact, from global databases, there is evidence that the fraction of nitrogen invested in the photosynthetic machinery and the slope of N_m vs. A_m relationships decreases with increasing leaf mechanical robustness (Niinemets, 1999; Onoda et al., 2017; Reich, Kloeppel, Ellsworth, & Walters, 1995). These studies together with our observations suggest that leaf trait variation at the low return end of the economics spectrum can result in suites of trait combinations that might deviate from the universal relationships. This deviation uncovered here emphasizes the importance of tree and needle age and species effects in altering mesophyll diffusion conductance and distribution of nitrogen among photosynthetic and non-photosynthetic functions, and ultimately foliage nitrogen use efficiency.

5 | CONCLUSIONS

This study highlights major differences in foliage photosynthetic characteristics among primary needles in young plants and secondary needles in mature plants and demonstrates that these differences primarily result from differences in foliage structure. Less robust foliage of juvenile needles is associated with greater photosynthetic activity per unit biomass investment. This that contributes to enhanced growth and seedling establishment, whereas the advantage of greater mechanical robustness of secondary needles in adult trees is tolerance of harsh environmental conditions in the upper canopy. However, as this study demonstrates, the inherent trade-off of greater mechanical resistance is a reduced fraction of needle biomass in photosynthetic tissues and lower mesophyll diffusion conductance. As the result of greater diffusion limitations, any given nitrogen investment in photosynthetic machinery results in lower photosynthetic returns in more robust needles.

Tree age- and needle age-dependent modifications in needle photosynthetic traits were qualitatively similar, indicating that increasingly sclerophyllous needle structure in older trees and in ageing needles has the same basic effects on foliage photosynthesis. However, as hypothesized, age-dependent changes in needle photosynthesis were less than differences due to tree age (Table 1), indicating that juvenile-to-adult transition is a much more profound change in needle functioning.

It has been suggested that due to large evolutionary and plastic modifications in foliar structure, structural limitations of foliar photosynthesis play at least as significant role as physiological and biochemical constraints (Niinemets & Sack, 2006). In the case of pine species studied here, heteroblasty and needle age, two characteristic sources of trait variation in conifers, produced an extensive continuum of variation in photosynthetic and structural traits, but limited variation in foliage nitrogen content. This resulted in several trait relationships deviating from the global leaf economics spectrum, suggesting that increases in leaf robustness can alter foliage photosynthetic activity not only due to changes in tissue chemical

composition, but also due to changes in mesophyll conductance and changes in the share of nitrogen between photosynthetic and non-photosynthetic functions.

ACKNOWLEDGEMENTS

Financial support for this research was provided by grants from the Consejo Superior de Investigaciones Cientificas (CSIC, Spain) and the Estonian Academy of Sciences (a grant for collaboration between scientific institutions of Estonia and CSIC), the Estonian Ministry of Science and Education (institutional grant IUT-8-3) and the European Commission through the European Regional Fund (the Center of Excellence EcolChange).

AUTHORS' CONTRIBUTIONS

Ü.N. and F.V. proposed the initial hypothesis, F.V. and V.K. made the experimental plan, V.K. carried out the experimental work, V.K. and Ü.N. analysed the data, V.K. and Ü.N. wrote the first draft of the MS, and all authors contributed to the subsequent versions of the MS and approved the final version of the study.

DATA ACCESSIBILITY

The data accompanying this article have been archived in the Dryad Digital Repository under https://doi.org/10.5061/dryad.hs20gv7 (Kuusk et al., 2018a).

ORCID

Ülo Niinemets http://orcid.org/0000-0002-3078-2192

REFERENCES

Bernacchi, C. J., Singsaas, E. L., Pimentel, C., Portis, A. R. Jr, & Long, S. P. (2001). Improved temperature response functions for models of Rubisco-limited photosynthesis. *Plant, Cell and Environment*, *24*, 253–259. https://doi.org/10.1111/j.1365-3040.2001.00668.x

Boddi, S., Bonzi, L. M., & Calamassi, R. (2002). Structure and ultrastructure of *Pinus halepensis* primary needles. *Flora*, *197*, 10–23. https://doi.org/10.1078/0367-2530-00008

Braza, R., & García, M. B. (2011). Spreading recruitment over time to cope with environmental variability. *Plant Ecology*, *212*, 283–292. https://doi.org/10.1007/s11258-010-9821-y

Climent, J., Aranda, I., Alonso, J., Pardos, J. A., & Gil, L. (2006). Developmental constraints limit the response of Canary Island pine seedlings to combined shade and drought. *Forest Ecology and Management*, *231*, 164–168. https://doi.org/10.1016/j.foreco.2006.05.042

Climent, J., Chambel, M. R., Pardos, M., Lario, F., & Villar-Salvador, P. (2011). Biomass allocation and foliage heteroblasty in hard pine species respond differentially to reduction in rooting volume. *European Journal of Forest Research*, *130*, 841–850. https://doi.org/10.1007/s10342-010-0476-y

Climent, J., San-Martín, R., Chambel, M. R., & Mutke, S. (2011). Ontogenetic differentiation between Mediterranean and Eurasian pines (sect. *Pinus*) at the seedling stage. *Trees: Structure and Function*, *25*, 175–186. https://doi.org/10.1007/s00468-010-0496-8

Day, M. E., Greenwood, M. S., & White, A. S. (2001). Age-related changes in foliar morphology and physiology in red spruce and their influence on declining photosynthetic rates and productivity with tree age. *Tree Physiology*, *21*, 1195–1204. https://doi.org/10.1093/treephys/21.16.1195

Diemer, M., Körner, C., & Prock, S. (1992). Leaf life spans in wild perennial herbaceous plants: A survey and attempts at a functional interpretation. *Oecologia*, *89*, 10–16. https://doi.org/10.1007/BF00319009

Dong, T., Li, J., Zhang, Y., Korpelainen, H., Niinemets, Ü., & Li, C. (2015). Partial shading of lateral branches affects growth, and foliage nitrogen- and water-use efficiencies in the conifer *Cunninghamia lanceolata* growing in a warm monsoon climate. *Tree Physiology*, *35*, 632–643. https://doi.org/10.1093/treephys/tpv036

Ethier, G. J., Livingston, N. J., Harrison, D. L., Black, T. A., & Moran, J. A. (2006). Low stomatal and internal conductance to CO_2 versus Rubisco deactivation as determinants of the photosynthetic decline of ageing evergreen leaves. *Plant, Cell and Environment*, *29*, 2168–2184. https://doi.org/10.1111/j.1365-3040.2006.01590.x

Evans, J. R., & Loreto, F. (2000). Acquisition and diffusion of CO_2 in higher plant leaves. In R. C. Leegood, T. D. Sharkey, & S. von Caemmerer (Eds.), *Photosynthesis: Physiology and metabolism* (pp. 321–351). Dordrecht, The Netherlands: Kluwer Academic. https://doi.org/10.1007/0-306-48137-5

Farquhar, G. D., von Caemmerer, S., & Berry, J. A. (1980). A biochemical model of photosynthetic CO_2 assimilation in leaves of C_3 species. *Planta*, *149*, 78–90. https://doi.org/10.1007/BF00386231

Gebauer, R., Volařík, D., Urban, J., Børja, I., Nagy, N. E., Eldhuset, T. D., & Krokene, P. (2011). Effect of thinning on anatomical adaptations of Norway spruce needles. *Tree Physiology*, *31*, 1103–1113. https://doi.org/10.1093/treephys/tpr081

Genty, B., Briantais, J.-M., & Baker, N. R. (1989). The relationship between the quantum yield of photosynthetic electron transport and quenching of chlorophyll fluorescence. *Biochimica et Biophysica Acta*, *990*, 87–92. https://doi.org/10.1016/S0304-4165(89)80016-9

Greenwood, M. S., Ward, M. H., Day, M. E., Adams, S. L., & Bond, B. J. (2008). Age-related trends in red spruce foliar plasticity in relation to declining productivity. *Tree Physiology*, *28*, 225–232. https://doi.org/10.1093/treephys/28.2.225

Harley, P. C., Loreto, F., di Marco, G., & Sharkey, T. D. (1992). Theoretical considerations when estimating the mesophyll conductance to CO_2 flux by analysis of the response of photosynthesis to CO_2. *Plant Physiology*, *98*, 1429–1436. https://doi.org/10.1104/pp.98.4.1429

Harper, J. L. (1989). The value of a leaf. *Oecologia*, *80*, 53–58. https://doi.org/10.1007/BF00789931

Hikosaka, K., & Shigeno, A. (2009). The role of Rubisco and cell walls in the interspecific variation in photosynthetic capacity. *Oecologia*, *160*, 443–451. https://doi.org/10.1007/s00442-009-1315-z

Jensen, A. M., Warren, J. M., Hanson, P. J., Childs, J., & Wullschleger, S. D. (2015). Needle age and season influence photosynthetic temperature response and total annual carbon uptake in mature *Picea mariana* trees. *Annals of Botany*, *116*, 821–832. https://doi.org/10.1093/aob/mcv115

Juárez-López, F. J., Escudero, A., & Mediavilla, S. (2008). Ontogenetic changes in stomatal and biochemical limitations to photosynthesis of two co-occurring Mediterranean oaks differing in leaf life span. *Tree Physiology*, *28*, 367–374. https://doi.org/10.1093/treephys/28.3.367

Karban, R., & Thaler, J. S. (1999). Plant phase change and resistance to herbivory. *Ecology*, *80*, 510–517. https://doi.org/10.1890/0012-9658(1999)080[0510:PPCART]2.0.CO;2

Kattge, J., Díaz, S., Lavorel, S., Prentice, C., Leadley, P., Bönisch, G., … Wirth, C. (2011). TRY – A global database of plant traits. *Global Change Biology*, *17*, 2905–2935. https://doi.org/10.1111/j.1365-2486.2011.02451.x

Keenan, T. F., & Niinemets, Ü. (2016). Global leaf trait estimates biased due to plasticity in the shade. *Nature Plants*, *3*, 16201. https://doi.org/10.1038/nplants.2016.201

Kuusk, V., Niinemets, Ü., & Valladares, F. (2018a). Data from: Structural controls on photosynthetic capacity through juvenile-to-adult transition and needle ageing in Mediterranean pines. *Dryad Digital Repository*, https://doi.org/10.5061/dryad.hs20gv7

Kuusk, V., Niinemets, Ü., & Valladares, F. (2018b). A major trade-off between structural and photosynthetic investments operative across plant and needle ages in three Mediterranean pines. *Tree Physiology* (in press). https://doi.org/10.1093/treephys/tpx1139

Mediavilla, S., Herranz, M., González-Zurdo, P., & Escudero, A. (2014). Ontogenetic transition in leaf traits: A new cost associated with the increase in leaf longevity. *Journal of Plant Ecology*, *7*, 567–575. https://doi.org/10.1093/jpe/rtt059

Miller, P. M., Eddleman, L. E., & Miller, J. M. (1995). *Juniperus occidentalis* juvenile foliage: Advantages and disadvantages for a stress-tolerant, invasive conifer. *Canadian Journal of Forest Research*, *25*, 470–479. https://doi.org/10.1139/x95-052

Niinemets, Ü. (1999). Research review. Components of leaf dry mass per area –thickness and density – alter leaf photosynthetic capacity in reverse directions in woody plants. *The New Phytologist*, *144*, 35–47. https://doi.org/10.1046/j.1469-8137.1999.00466.x

Niinemets, Ü. (2002). Stomatal conductance alone does not explain the decline in foliar photosynthetic rates with increasing tree age and size in *Picea abies* and *Pinus sylvestris*. *Tree Physiology*, *22*, 515–535. https://doi.org/10.1093/treephys/22.8.515

Niinemets, Ü. (2014). Improving modeling of the "dark part" of canopy carbon gain. *Tree Physiology*, *34*, 557–563. https://doi.org/10.1093/treephys/tpu030

Niinemets, Ü. (2015). Is there a species spectrum within the world-wide leaf economics spectrum? Major variations in leaf functional traits in the Mediterranean sclerophyll *Quercus ilex*. *The New Phytologist*, *205*, 79–96. https://doi.org/10.1111/nph.13001

Niinemets, Ü., Cescatti, A., Rodeghiero, M., & Tosens, T. (2005). Leaf internal diffusion conductance limits photosynthesis more strongly in older leaves of Mediterranean evergreen broad-leaved species. *Plant, Cell and Environment*, *28*, 1552–1566. https://doi.org/10.1111/j.1365-3040.2005.01392.x

Niinemets, Ü., Díaz-Espejo, A., Flexas, J., Galmés, J., & Warren, C. R. (2009). Role of mesophyll diffusion conductance in constraining potential photosynthetic productivity in the field. *Journal of Experimental Botany*, *60*, 2249–2270. https://doi.org/10.1093/jxb/erp036

Niinemets, Ü., García-Plazaola, J. I., & Tosens, T. (2012). Photosynthesis during leaf development and ageing. In J. Flexas, F. Loreto & H. Medrano (Eds.), *Terrestrial photosynthesis in a changing environment. A molecular, physiological and ecological approach* (pp. 353–372). Cambridge, UK: Cambridge University Press. https://doi.org/10.1017/CBO9781139051477

Niinemets, Ü., Hauff, K., Bertin, N., Tenhunen, J. D., Steinbrecher, R., & Seufert, G. (2002). Monoterpene emissions in relation to foliar photosynthetic and structural variables in Mediterranean evergreen *Quercus* species. *The New Phytologist*, *153*, 243–256. https://doi.org/10.1046/j.0028-646X.2001.00323.x

Niinemets, Ü., Keenan, T. F., & Hallik, L. (2015). Tansley review. A worldwide analysis of within-canopy variations in leaf structural, chemical and physiological traits across plant functional types. *The New Phytologist*, *205*, 973–993. https://doi.org/10.1111/nph.13096

Niinemets, Ü., & Kull, O. (1995). Effects of light availability and tree size on the architecture of assimilative surface in the canopy of *Picea abies*: Variation in needle morphology. *Tree Physiology*, *15*, 307–315. https://doi.org/10.1093/treephys/15.5.307

Niinemets, Ü., & Sack, L. (2006). Structural determinants of leaf light-harvesting capacity and photosynthetic potentials. In K. Esser, U. E. Lüttge, W. Beyschlag, & J. Murata (Eds.), *Progress in botany* (pp. 385–419). Berlin, Germany: Springer. https://doi.org/10.1007/3-540-27998-9

Niinemets, Ü., & Tenhunen, J. D. (1997). A model separating leaf structural and physiological effects on carbon gain along light gradients for the shade-tolerant species *Acer saccharum*. *Plant, Cell and Environment*, *20*, 845–866. https://doi.org/10.1046/j.1365-3040.1997.d01-133.x

Niinemets, Ü., Wright, I. J., & Evans, J. R. (2009). Leaf mesophyll diffusion conductance in 35 Australian sclerophylls covering a broad range of foliage structural and physiological variation. *Journal of Experimental Botany*, *60*, 2433–2449. https://doi.org/10.1093/jxb/erp045

Oleksyn, J., Tjoelker, M. G., Lorenc-Plucińska, G., Konwińska, A., Żytkowiak, R., Karolewski, P., & Reich, P. B. (1997). Needle CO_2 exchange, structure and defence traits in relation to needle age in *Pinus heldreichii* Christ – a relict of Tertiary flora. *Trees: Structure and Function*, *12*, 82–89.

Onoda, Y., Wright, I. J., Evans, J. R., Hikosaka, K., Kitajima, K., Niinemets, Ü., … Westoby, M. (2017). Physiological and structural tradeoffs underlying the leaf economics spectrum. *The New Phytologist*, *214*, 1447–1463. https://doi.org/10.1111/nph.14496

Pardos, M., Calama, R., & Climent, J. (2009). Difference in cuticular transpiration and sclerophylly in juvenile and adult pine needles relates to the species-specific rates of development. *Trees: Structure and Function*, *23*, 501–508. https://doi.org/10.1007/s00468-008-0296-6

Peñuelas, J., Sardans, J., Llusià, J., Owen, S. M., Carnicer, J., Giambelluca, T. W., … Niinemets, Ü. (2010). Faster returns on 'leaf economics' and different biogeochemical niche in invasive compared with native plant species. *Global Change Biology*, *16*, 2171–2185.

Poorter, H., Niinemets, Ü., Poorter, L., Wright, I. J., & Villar, R. (2009). Tansley review. Causes and consequences of variation in leaf mass per area (LMA): A meta-analysis. *The New Phytologist*, *182*, 565–588. https://doi.org/10.1111/j.1469-8137.2009.02830.x

Prévosto, B., Gavinet, J., Ripert, C., & Fernandez, C. (2015). Identification of windows of emergence and seedling establishment in a pine Mediterranean forest under controlled disturbances. *Basic and Applied Ecology*, *16*, 36–45. https://doi.org/10.1016/j.baae.2014.10.008

R Development Core Team. (2012). *R: A language and environment for statistical computing*. Vienna, Austia: The R Foundation for Statistical Computing.

Räim, O., Kaurilind, E., Hallik, L., & Merilo, E. (2012). Why does needle photosynthesis decline with tree height in Norway spruce? *Plant Biology*, *14*, 306–314. https://doi.org/10.1111/j.1438-8677.2011.00503.x

Reich, P. B. (1993). Reconciling apparent discrepancies among studies relating life span, structure and function of leaves in contrasting plant life forms and climates: 'The blind men and the elephant retold'. *Functional Ecology*, *7*, 721–725. https://doi.org/10.2307/2390194

Reich, P. B., Kloeppel, B. D., Ellsworth, D. S., & Walters, M. B. (1995). Different photosynthesis-nitrogen relations in deciduous hardwood and evergreen coniferous tree species. *Oecologia*, *104*, 24–30. https://doi.org/10.1007/BF00365558

Rodeghiero, M., Niinemets, Ü., & Cescatti, A. (2007). Major diffusion leaks of clamp-on leaf cuvettes still unaccounted: How erroneous are the estimates of Farquhar *et al*. model parameters? *Plant, Cell and Environment*, *30*, 1006–1022. https://doi.org/10.1111/j.1365-3040.2007.001689.x

Steppe, K., Niinemets, Ü., & Teskey, R. O. (2011). Tree size- and age-related changes in leaf physiology and their influence on carbon gain. In F. C. Meinzer, T. Dawson, & B. Lachenbruch (Eds.), *Size- and age-related changes in tree structure and function* (pp. 235–253). Berlin, Germany: Springer. https://doi.org/10.1007/978-94-007-1242-3

Takashima, T., Hikosaka, K., & Hirose, T. (2004). Photosynthesis or persistence: Nitrogen allocation in leaves of evergreen and deciduous *Quercus* species. *Plant, Cell and Environment*, *27*, 1047–1054. https://doi.org/10.1111/j.1365-3040.2004.01209.x

Teskey, R. O., Grier, C. C., & Hinckley, T. M. (1984). Change in photosynthesis and water relations with age and season in *Abies*

amabilis. *Canadian Journal of Forest Research*, *14*, 77–84. https://doi.org/10.1139/x84-015

Tissue, D. T., Griffin, K. L., Turnbull, M. H., & Whitehead, D. (2001). Canopy position and needle age affect photosynthetic response in field-grown *Pinus radiata* after five years of exposure to elevated carbon dioxide partial pressure. *Tree Physiology*, *21*, 915–923. https://doi.org/10.1093/treephys/21.12-13.915

Tomás, M., Flexas, J., Copolovici, L., Galmés, J., Hallik, L., Medrano, H., … Niinemets, Ü. (2013). Importance of leaf anatomy in determining mesophyll diffusion conductance to CO_2 across species: Quantitative limitations and scaling up by models. *Journal of Experimental Botany*, *64*, 2269–2281. https://doi.org/10.1093/jxb/ert086

Tosens, T., Niinemets, Ü., Westoby, M., & Wright, I. J. (2012). Anatomical basis of variation in mesophyll resistance in eastern Australian sclerophylls: News of a long and winding path. *Journal of Experimental Botany*, *63*, 5105–5119. https://doi.org/10.1093/jxb/ers171

Veromann, L.-L., Tosens, T., Laanisto, L., & Niinemets, Ü. (2017). Extremely thick cell walls and low mesophyll conductance: Welcome to the world of ancient living! *Journal of Experimental Botany*, *68*, 1639–1653. https://doi.org/10.1093/jxb/erx045

von Caemmerer, S., & Farquhar, G. D. (1981). Some relationships between the biochemistry of photosynthesis and the gas exchange of leaves. *Planta*, *153*, 376–387. https://doi.org/10.1007/BF00384257

Warren, C. R. (2006). Why does photosynthesis decrease with needle age in *Pinus pinaster*? *Trees: Structure and Function*, *20*, 157–164. https://doi.org/10.1007/s00468-005-0021-7

Warren, C. R., & Adams, M. A. (2000). Trade-offs between the persistence of foliage and productivity in two Pinus species. *Oecologia*, *124*, 487–494. https://doi.org/10.1007/PL00008874

Way, D. A., & Yamori, W. (2014). Thermal acclimation of photosynthesis: On the importance of adjusting our definitions and accounting for thermal acclimation of respiration. *Photosynthesis Research*, *119*, 89–100. https://doi.org/10.1007/s11120-013-9873-7

Weiskittel, A. R., Temesgen, H., Wilson, D. S., & Maguire, D. A. (2008). Sources of within- and between-stand variability in specific leaf area of three ecologically distinct conifer species. *Annals of Forest Science*, *65*, 103. https://doi.org/10.1051/forest:2007075

Woodruff, D. R., Meinzer, F. C., Lachenbruch, B., & Johnson, D. M. (2009). Coordination of leaf structure and gas exchange along a height gradient in a tall conifer. *Tree Physiology*, *29*, 261–272.

Wright, I. J., Groom, P. K., Lamont, B. B., Poot, P., Prior, L. D., Reich, P. B., … Westoby, M. (2004). Leaf trait relationships in Australian plant species. *Functional Plant Biology*, *31*, 551–558. https://doi.org/10.1071/FP03212

Wright, I. J., Reich, P. B., Westoby, M., Ackerly, D. D., Baruch, Z., Bongers, F., … Villar, R. (2004). The world-wide leaf economics spectrum. *Nature*, *428*, 821–827. https://doi.org/10.1038/nature02403

Yoder, B. J., Ryan, M. G., Waring, R. H., Schoettle, A. W., & Kaufmann, M. R. (1994). Evidence of reduced photosynthetic rates in old trees. *Forest Science*, *40*, 513–527.

Zotz, G., Wilhelm, K., & Becker, A. (2011). Heteroblasty – A review. *Botanical Review*, *77*, 109–151. https://doi.org/10.1007/s12229-010-9062-8

SUPPORTING INFORMATION

Additional Supporting Information may be found online in the supporting information tab for this article.

How to cite this article: Kuusk V, Niinemets Ü, Valladares F. Structural controls on photosynthetic capacity through juvenile-to-adult transition and needle ageing in Mediterranean pines. *Funct Ecol*. 2018;32:1479–1491. https://doi.org/10.1111/1365-2435.13087